1st International Conference "From Scientific Computing to Computational Engineering"
1st IC-SCCE
Athens, 8-10 September, 2004

SMART PASSIVE SYSTEM BASED ON MR DAMPER

Sang-Won Cho*, Kyu-Sik Park*, Chun-Ho Kim†, and In-Won Lee*

* Structural Dynamics and Vibration Control Laboratory (SDVCL)
Korea Advanced Institute of Science and Technology (KAIST)
e-mail: s.w.cho@kaist.ac.kr, web page: http://sdvc.kaist.ac.kr

†Joongbu University

Keywords: MR damper, Semi-active, Passive, Control, Electromagnetic induction.

Abstract. *Magnetorheological (MR) dampers are one of the most promising control devices for civil engineering applications to earthquake hazard mitigation, because they have many advantages such as small power requirement, reliability, and low price to manufacture. To reduce the responses of the controlled structure by using MR dampers, a control system including power supply, controller, and sensors is needed. However, it is not easy to apply the MR damper-based control system to large-scale civil structures, such as cable-stayed bridges and high-rise buildings, because of the difficulties of building up and maintaining the control system. This paper proposes a MR damper with an electromagnetic induction (EMI) system for a civil engineering application, which consists of a permanent magnet and a coil. According to the Faraday's law of induction, the EMI system changes kinetic energy of a MR damper to electric energy and then electric energy is used to vary the damping characteristics of the MR damper. It is easy to build up and maintain the proposed MR damper with the EMI system, because it does not require any control system such as a power supply, controller, and sensors. To verify the effectiveness of the proposed EMI system, the performances are compared with those of the normal MR damper. The numerical results show that the MR damper with the EMI system has the comparable performance to the normal MR damper system.*

1 INTRODUCTION

Magnetorheological (MR) dampers are one of the semi-active control devices, which use MR fluids to provide controllable damping forces. Since B.F. Spencer first introduced MR dampers to civil engineering applications in mid 1990s, MR dampers have received considerable attention, because of its mechanical simplicity, high dynamic range, low operating power requirements, large force capacity, and environmental robustness (Kamath and Wereley 1997; Dyke and Spencer 1996; Ginder et al. 1996; Spencer et al. 1997a; Spencer and Sain 1997; Dyke et al. 1998). In 2001, a MR damper was applied to the cable-stayed Dongting Lake Bridge in China and the Nihon-Kagaku-Miraikan building in Japan for reduction of responses of the structures, which are the world's first full-scale implementations in civil engineering structures.

To reduce the responses of controlled structure, a MR damper needs a control system including a power supply such as a battery and a controller to determine the control commands using the measured responses from sensors. However, it is not easy to apply the MR damper based control system to large-scale civil structures such as cable-stayed brides and high-rise buildings. In those cases, many MR dampers are used and each MR damper is connected to one or more power supplies and controllers. Also, many sensors are needed to measure the structural responses to determine the control commands for each MR damper. Therefore, it is difficult to build up and maintain the MR damper based control system, especially when it is used for large-scale civil structures.

In this paper, an electromagnetic induction (EMI) system is newly adopted to MR dampers to replace a control system including a power supply, a controller, and sensors. The EMI system consists of a permanent magnet and a coil. According to the Faraday's law of induction (Reitz et. al. 1993; Marshall and Skitek 1990; Miner 1996), the EMI system changes kinetic energy of reciprocation motion of the MR damper to electric energy and then electric energy is used to change the damping characteristics of MR fluid. In addition, fast motions of the MR damper induce high current and slow relative motions induce low current at the EMI system, which can adapt MR damper to the various external excitations like earthquakes. In brief, MR damper is powered and controlled by the EMI system. Therefore, the proposed MR damper with the EMI system is easy to build up and maintain, because it does not require any power supply, controller and sensors. This is an important benefit of using the MR damper with the EMI system. An EMI system was adopted to control an engine mount

of the vehicle (Korea patent 2000-004066) and to control an electrorheological (ER) damper (Japan patent 2-145337). This paper focuses on civil engineering applications of the MR damper with the EMI system. To investigate the achievable capabilities of the proposed MR damper with the EMI system, the EMI system is designed. Then, the effectiveness of performances are evaluated and compared with those of a normal MR damper system using the clipped-optimal controller.

2 MR DAMPER WITH THE EMI SYSTEM

A prototype MR damper has been considered to show the schematic of MR dampers, which was obtained for evaluation from the Lord Corporation and was used by Dyke et al.(1996a). The damper is 21.5 cm long in its extended position, and the main cylinder is 3.8 cm diameter. The main cylinder houses the piston, the electromagnet, an accumulator and 50 ml of MR fluid, and the damper has a ±2.5 cm stroke. As shown in Fig. 1, the magnetic field produced in the device is generated by a small electromagnet in the piston head. The current for the electromagnet is supplied by a power supply such as a battery and regulated by a controller which determines control commands, resulting in changes of damping characteristics of MR fluid. Thus, to reduce the structural responses, The MR damper needs a control system that consists of a power supply, a controller, and sensors. Although the MR damper-based control system is simple, many MR dampers are used for civil engineering structures such as cable-stayed bridges and high-rise buildings. In that case, the MR damper based control system becomes more complicated to build up and maintain.

An electromagnetic induction (EMI) system is newly adopted to MR dampers to replace a control system. Fig. 2 shows the MR damper with the EMI system that consists of a permanent magnet and a coil. The EMI system changes kinetic energy of reciprocation motion of MR damper to electric energy according to the Faraday's law of induction (Reitz et. al. 1993; Marshall and Skitek 1990; Miner 1996) and then electric energy is used to change the damping characteristics of MR damper. The characteristics of MR fluid is affected by magnetic field. The magnetic fields at coil 1 solidify MR fluid resulting increase of damping capacity of damper. The magnetic field is arisen by induced current of the EMI system (consists of permanent magnet and coil 2). Fast relative motions between permanent magnet and coil 2 make high current at coil 1. Slow relative motions between permanent magnet and coil 2 make low current at coil 1. Thus, MR damper with the EMI system is able to reduce the vibrations of structures by itself without any power supply and controller.

Faraday's law of induction is

$$\varepsilon = -N \frac{d\Phi_B}{dt} \tag{1}$$

where ε is induced electromotive force(emf) that has unit of volt(V), N is number of turns of coil, and Φ_B is magnetic flux. Negative sign in Eq.(1) is the direction of induced current. In Eq.(1), magnet flux can be defined

$$d\Phi_B = \vec{B} \cdot d\vec{A} = BdA \cdot \cos\phi \tag{2}$$

where $\vec{B}$ is magnetic field, $\vec{A}$ is area of cross section, and ϕ is the angle between $\vec{B}$ and $d\vec{A}$. Using Eq.(2), Faraday's law can be rewritten

$$\varepsilon = -N \frac{d\Phi_B}{dt} = -N A \frac{dB}{dt} \tag{3}$$

Faraday's law of induction states that the induced emf in a closed loop equals the negative of the time rate of change of magnetic flux through the loop. External loads such as earthquakes and winds cause the reciprocal motion of MR damper. In consequence, the coil in the EMI system at the end of the piston-axle moves back and forth inducing the emf. Thus, the faster MR damper moves, the higher emf is induced and the slower MR damper moves, the lower emf is induced. This induced emf is carried to an electromagnet in the piston head and generates magnetic field around electromagnet that changes damping characteristics of MR fluid.

To verify the feasibility of the proposed EMI system, we can estimate the maximum induced emf using Faraday's law for the prototype MR damper in Fig. 1. Provided that permanent magnet of 1.2 Tesla is used in the EMI system, the maximum velocity of reciprocal motion of the MR damper is 9cm/sec (that is about the maximum velocity of uncontrolled case of following numerical example), and the turns of coil are 900, then the time rate of change of magnetic field during the full stroke of 5cm is 2.16 Tesla/sec. The resulting emf induced in the coil is about 2.54V. Considering that saturation of the MR effect begins in the prototype device when the applied voltage is 2.25V, the maximum induced emf, 2,54V, is enough to change the damping characteristics of MR fluid. Besides, the amount of induced emf can be regulated by the turns of coil or the intensity of permanent magnet.

The proposed MR damper with the EMI system does not need sensors that measure structural responses for a controller, because the damping characteristics of MR damper is automatically regulated in proportion to the time rate of change of magnetic flux. Also, the power for electromagnet in piston head is supplied by induced emf of the EMI system, which means there is no need of a power supply. Therefore, the proposed MR damper with the EMI system can replace a conventional MR damper based control system. This is the important benefit of using MR damper with the EMI system.

3 ANALYTICAL MODEL AND DESIGN

3.1 Analytical model

The performances of the MR damper with the EMI system are now evaluated through simulations. A model of a three-story building configured with a single MR damper is considered here for direct comparisons with the normal MR damper, which is the exact one used by Dyke et al. (1996a). The MR damper is rigidly connected between the ground and the first floor of the structure.

The governing equations of the structure are given by

$$\dot{z} = Az + Bf + E\ddot{x}_g \tag{4}$$

where $\ddot{x}_g$ is a one-dimensional ground acceleration, f is the measured force generated between the structure and the MR damper, z is the state vector. The equations governing the force f predicted by this model were given by Spencer et al. (1997a).

3.2 Designing the EMI System

According to the Faraday's law of induction, the induced emf is proportional to the turns of the coil and the time rate of change of magnetic flux. Thus, the amount of emf can be regulated by the turns of the coil with a fixed capacity of permanent magnet. Appropriate number of coil turns needs to be determined in the design for better performance of the MR damper with the EMI system. In the design of the EMI system for this study, the influence of two parameters is considered: S_a, the summation of peak accelerations and S_i, the summation of peak inter-drift displacements at each floor, which are normalized by uncontrolled responses, respectively. To determine the coil turns, maximum response approach (Park et al. 2003) is used for parameters S_a and S_i with three earthquakes, El Centro, Hachinohe and Kobe earthquakes.

Fig. 3(a) shows the variations of S_a for each earthquake and Fig. 3(b) is the envelope of the maximum responses of Fig. 3(a). From Fig. 3(b), we can determine the optimal coil turns, which is the minimum point of the envelope denoted by arrow. Fig. 4 is similar to Fig. 3 except that it is for S_i. Two appropriate coil turns, 2.16×10^4 and 2.6×10^4 (turns/m), are determined from the Figs. 3 and 4. Finally, an EMI system, designed for S_a, is designated EMI_{ac} and the other EMI system, designed for S_i, is called EMI_{dr}.

For the comparison of the performance, a normal MR damper system using the clipped optimal controller (Dyke et al. 1996a,b) is considered. Two sets of appropriate weighting parameter, $q_a=5.0\times10^{-13}$, $q_i=1.0\times10^{-5}$ for S_a and $q_a=5.0\times10^{-15}$, $q_i=5.0\times10^{-6}$ for S_i, are determined. The clipped-optimal controller, designed for S_a, with weighting parameters q_a and q_i, is designated CO_{ac} and the other, designed for S_i, is called CO_{dr}.

4 NUMERICAL SIMULATIONS RESULTS

To verify the effectiveness of the proposed MR damper with the EMI system, a set of simulations is performed for the four historical earthquakes such as El Centro, Hachinohe, Kobe, and Northridge earthquakes. The Northridge earthquake is not considered in the designing phase, but is included here to check the validation of the design of the EMI system and the clipped-optimal controller. Simulation results of the proposed EMI system are compared to those of the normal MR damper system using the clipped optimal controller by evaluation criteria based on those used in the second generation linear control problem for buildings (Spencer et al., 1997b). The first evaluation criterion is a measure of the normalized peak floor accelerations, given by

$$J_1 = \max_{t,i}\left(\frac{|\ddot{x}_{ai}(t)|}{\ddot{x}_a^{\max}}\right),\ J_2 = \max_{t,i}\left(\frac{|d_i(t)|}{d_n^{\max}}\right) \tag{5}$$

where the absolute accelerations of the ith floor, $\ddot{x}_{ai}(t)$, are normalized by the peak uncontrolled floor

acceleration, denoted $\ddot{x}_a^{\max}(t)$, and $d_i(t)$ is the inter-story drift of the above ground floors over the response history, and $d_n^{\max}$ denotes the normalized peak inter-story drift in the uncontrolled response.

Representative responses of the EMI system to four earthquakes are shown in graphs. Fig. 5 shows the velocities at the first floor where the MR damper is attached and the induced voltages by the EMI system under El Centro earthquake. For moderate earthquakes (El Centro and Hachinohe), the velocity of the first floor is smaller than that of severe earthquakes (Kobe and Northridge) with the consequence that the induced voltage by the EMI system is lower according to the Faraday's law of induction. Also, it can be seen that the higher voltage is induced for severe earthquakes. The maximum induced voltage is 1.6V, 0.9V, 2.25V, and 2.25V for El Centro, Hachinohe, Kobe, and Northridge earthquakes, respectively, which is the voltage enough to be able to operate the MR damper. Besides, it should be noted that the induced voltage is restricted within 2.25V for the capacity of the MR damper, which is identical condition with the clipped-optimal controller. However, the induced voltage is continuously varying whereas the command voltage of the clipped-optimal controller takes on values of either zero or the maximum value.

Table 1 shows the accelerations and the inter-story drifts at each floor for four cases of two categories (i.e., EMI_{ac}, EMI_{dr}, CO_{ac}, and CO_{dr}) normalized by each uncontrolled response, respectively. The colored cells are the minimum value among four cases at each floor. The clipped-optimal controllers achieve more reductions over the EMI systems for the moderate earthquakes such as El Centro and Hachinohe, except that the EMI systems give minimum value at the first floor. For the severe earthquakes such as Kobe and Northridge, however, the performances of the EMI system are better than those of the clipped-optimal controller giving 35.5% and 24.1% additional decreases in maximum in the peak acceleration and inter-story drift, respectively, compared to the better clipped-optimal controller. Though the EMI system fails to achieve more reductions over the clipped-optimal controller for the moderate earthquakes, it has comparable performance to the clipped-optimal controller without the power source, controller, and sensors. This is the important benefit of using the MR damper with the EMI system.

5 CONCLUDING REMARKS

This paper has proposed the MR damper with the EMI system for a civil engineering application. The EMI system consists of a permanent magnet and a coil. According to the Faraday's law of induction, the EMI system generates induced voltages that can supply electricity and control commands to the MR damper, replacing a normal control system such as a power supply, a controller, and sensors.

To investigate the achievable capabilities of the MR damper with the EMI system, two EMI systems were designed. Then, the effectiveness of performances are evaluated, and compared with those of a normal MR damper system. In comparing both systems, it was observed that for the moderate earthquake such as El Centro and Hachinohe, the MR damper with the EMI system showed the comparable performance to the normal MR damper system. For the severe earthquakes such as Kobe and Northridge, the MR damper with the EMI system shows the better performance giving 35.5% and 24.1% additional maximum decreases in the peak acceleration and inter-story drift, respectively.

In addition to the comparable performance, the proposed MR damper with the EMI system has the simple structure without any power supply, controller, and sensors. Therefore, the Proposed MR damper with the EMI system has potential to be implemented in real civil structures. Further studies are underway to conduct a series of experiments in which numerical simulation results will be verified.

EFERENCES

[1] Dyke, S. J., and Spencer, B. F., Jr. (1996). ''Seismic response control using multiple MR dampers.'' Proc., 2nd Int. Workshop on Struc. control, Hong Kong University of Science and Technology Research Center, Hong, Kong, 163–173.

[2] Dyke, S.J., Spencer Jr., B.F., Sain, M.K. and Carlson, J.D. (1996a). "Modeling and Control of Magnetorheological Dampers for Seismic Response Reduction," Smart Materials and Structures, Vol. 5, pp. 565–575.

[3] Dyke, S.J., Spencer Jr., B.F., Sain, M.K. and Carlson, J.D. (1996b). "Seismic Response Reduction Using Magnetorheological Dampers." Proc. of the IFAC World Congress, San Francisco, CA, June 30–July 5.

[4] Dyke, S.J., Spencer Jr., B.F., Sain, M.K., and Carlson, J.D. (1998). "An Experimental Study of MR Dampers for Seismic Protection," Smart Materials and Structures: Special Issue on Large Civil Structures, Vol. 7, pp. 693–703.

[5] Ginder, J.M., Davis, L.C., and Elie, L.D. (1996). "Rheology of Magnetorheological Fluids: Models and Measurements," International Journal of Modern Physics B, Vol. 10, Nos. 23 & 24, pp. 3293-3303.

[6] Kamath, G.M, and Wereley, N.M. (1997). "A Nonlinear Viscoelastic-Plastic Model for Electrorheological

Fluids," Smart Materials and Structures, Vol. 6, No. 3.
[7] Marshall, S.V. and Skitek, G. G. (1990), Electromagnetic concepts and applications, Prentice Hall.
[8] Miner, G.F. (1996), Lines and electromagnetic fields for engineers, Oxford University Press.
[9] Reitz, J.R. Milford, F.J., and Christy R.W. (1993), Foundations of electromagnetic theory, Addison-Wesley Pub. Co.
[10] Park, K.S., Jung, H.J and Lee, I.W. (2003), "Hybrid Control Strategy for Seismic Protection of a Benchmark Cable-Stayed Bridge," Engineering Structures, Vol. 25, No. 4, pp. 405-417.
[11] Soong, T.T. (1990), Active Structural Control: Theory and Practice, Longman Scientific and Technical, Essex, England.
[12] Spencer Jr., B.F. and Sain, M.K. (1997). "Controlling Buildings: A New Frontier in Feedback," IEEE Control Systems Magazine: Special Issue on Emerging Technologies (Tariq Samad Guest Ed.), Vol. 17, No. 6, pp. 19-35.
[13] Spencer Jr., B.F., Dyke, S.J., Sain, M.K. and Carlson, J.D., (1997a). "Phenomenological Model of a Magnetorheological Damper," J. Engrg. Mech., ASCE, Vol. 123, No. 3, pp. 230-238.
[14] Spencer Jr., B.F., Dyke, S.J., Sain, M.K. and Carlson, J.D., (1997b). "Benchmark Problems in Structural Control – Part I: Active Mass Driver System," Proc. ASCE Struct. Congr. XV., ASCE, New York, pp. 1265-1269.

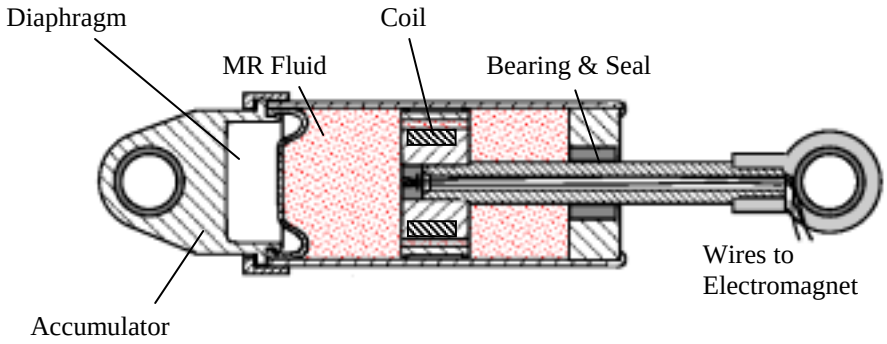

Figure 1. Schematic of a MR damper (Dyke et al. 1996a)

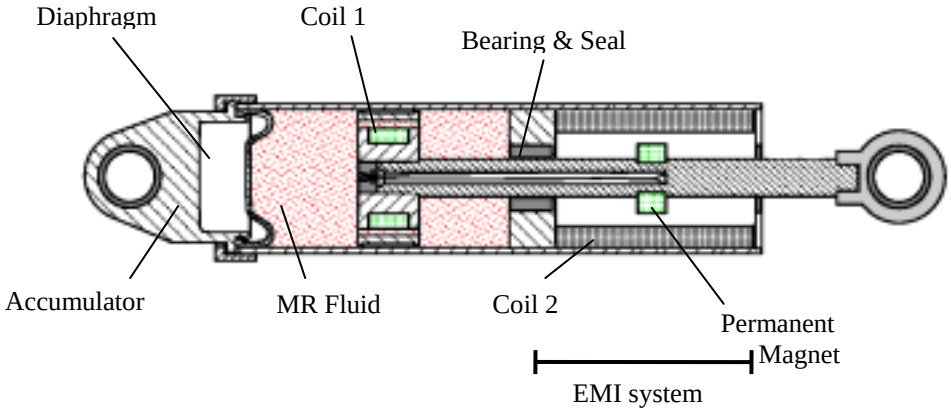

Figure 2. Schematic of a MR Damper with the EMI System

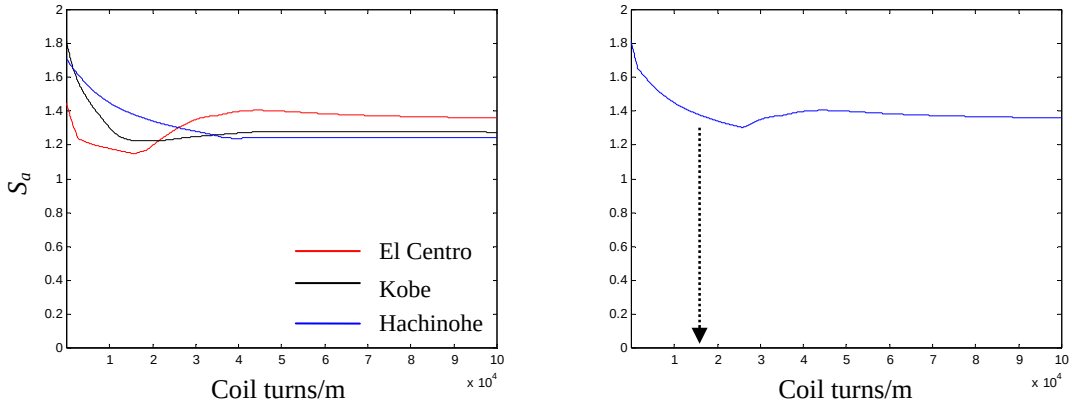

(a) Variations of Sa (b) Envelope of Max. Responses of (a)

Figure 3. Design of EMI System with Sa under Three Earthquakes

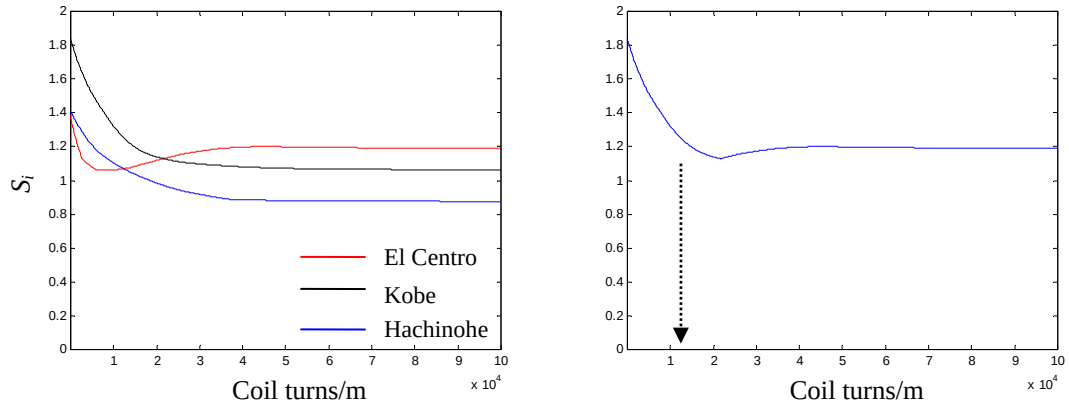

(a) Variations of S_i (b) Envelope of Max. Responses of (a)

Figure 4. Design of EMI System with Sa under Three Earthquakes

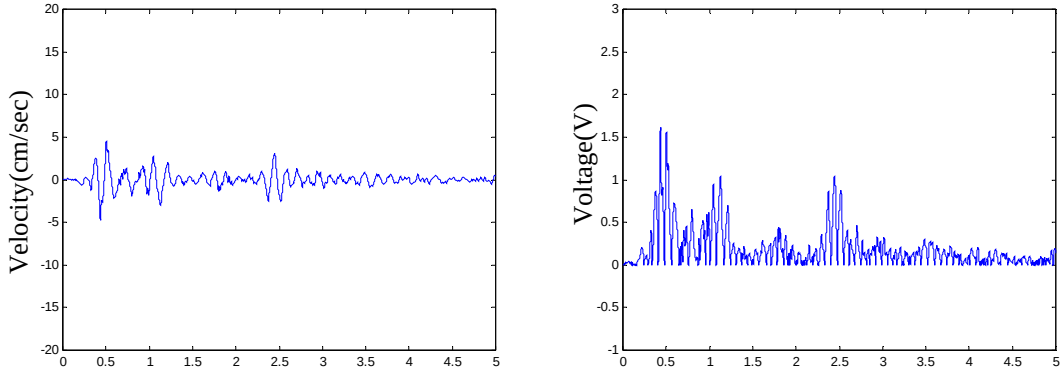

Figure 5. Velocities and Induced Voltages under El Centro Earthquake

Table 1 Normalized peak absolute accelerations and inter-story drifts

Story	Accelerations							
	El Centro (0.3495)*				Hachinohe (0.2294)			
	CO_{ac}	CO_{dr}	EMI_{ac}	EMI_{dr}	CO_{ac}	CO_{dr}	EMI_{ac}	EMI_{dr}
1st	0.499	0.551	0.355	0.340	0.492	0.515	0.372	0.377
2nd	0.354	0.433	0.436	0.396	0.431	0.520	0.526	0.530
3rd	0.441	0.473	0.512	0.492	0.384	0.465	0.404	0.423
Story	Kobe (0.8337)				Northridge (0.8428)			
	CO_{ac}	CO_{dr}	EMI_{ac}	EMI_{dr}	CO_{ac}	CO_{dr}	EMI_{ac}	EMI_{dr}
1st	0.370	0.429	0.367	0.345	0.897	0.881	0.568	0.568
2nd	0.494	0.493	0.484	0.485	0.587	0.554	0.612	0.586
3rd	0.410	0.384	0.387	0.393	0.815	0.800	0.725	0.738

Story	Inter-story Drifts							
	El Centro (0.3495)				Hachinohe (0.2294)			
	CO_{ac}	CO_{dr}	EMI_{ac}	EMI_{dr}	CO_{ac}	CO_{dr}	EMI_{ac}	EMI_{dr}
1st	0.228	0.212	0.168	0.180	0.295	0.243	0.178	0.194
2nd	0.423	0.448	0.476	0.457	0.289	0.319	0.357	0.355
3rd	0.441	0.473	0.512	0.492	0.384	0.465	0.404	0.423
~~Story~~	Kobe (0.8337)				Northridge (0.8428)			
	CO_{ac}	CO_{dr}	EMI_{ac}	EMI_{dr}	CO_{ac}	CO_{dr}	EMI_{ac}	EMI_{dr}
1st	0.348	0.308	0.293	0.301	0.563	0.473	0.359	0.382
2nd	0.456	0.442	0.428	0.435	0.859	0.846	0.827	0.835
3rd	0.410	0.384	0.387	0.393	0.815	0.800	0.725	0.738

* ( ) is peak ground acceleration (g)